Research Article

Fethi Bennour and Hocine Mzad*

A numerical investigation of optimum angles for solar energy receivers in the eastern part of Algeria

https://doi.org/10.1515/ehs-2021-0089
Received December 27, 2021; accepted August 21, 2022;
published online September 30, 2022

Abstract: The need to capture the maximum amount of solar energy and to optimize the panels' collecting surfaces are among the primary objectives of research in solar engineering. The simplest way to accomplish this is to perform a monthly accurate determination of the solar collector's proper slope and azimuth angles. Indeed, this is the aim of this article, which consists of a graphical optimization based on the Gueymard's daily integration model. A Matlab program was developed to predict the hourly solar radiation on a solar receiver using the Gueymard model in conjunction with the Liu and Jordan isotropic, Perez, and HDKR anisotropic models. A comprehensive simulation of the monthly solar irradiation throughout 2018 was executed for the city of Annaba, in north–eastern Algeria. The results indicate that the south-facing surface azimuth angle is the most appropriate. In fact, for maximum sunlight capture, the solar collector inclination must be adjusted each month in the range of [10–40°]. Furthermore, the results show that the gains in the amount of solar radiation received throughout the year by the thermal panel mounted at monthly optimum tilt angles are 15.63% in January and 7.37% in July.

Keywords: azimuth angle; Gueymard model; optimization; slope angle; solar collector; solar radiation.

***Corresponding author: Hocine Mzad**, Mechanical Engineering Department, Badji Mokhtar University, P.O. Box 12, DZ-23005, Annaba, Algeria, E-mail: h_mzad@yahoo.fr.
https://orcid.org/0000-0001-9900-6960
Fethi Bennour, Laboratory of Research on Industrial Risk Control and Safety, Badji Mokhtar University, P.O. Box 12, DZ-23005, Annaba, Algeria, E-mail: bennourfethi@yahoo.fr. https://orcid.org/0000-0002-8778-3014

Introduction

The fact that a large volume of meteorological radiation and temperature data must be analyzed has made the prediction of collector performance an extremely tedious task. It is, therefore, desirable to study the available radiation and temperature data and to correlate and present them in such a form that further detailed analysis of these data becomes unnecessary in the prediction of collector performance.

Methods for predicting the long-term average insolation available to solar correctors, both fixed and tracking, and of arbitrary orientation, have been described by Liu and Jordan (1963), Collares-Pereira and Rabl (1979), and Erbs, Klein, and Duffie (1982), recognized as the prediction models for collector performance. To apply these methods, a large volume of meteorological radiation and temperature data for the locality of the collector must be analyzed.

It is well known that the time when we can capture the maximum of solar radiation is between noon and 1 pm. The fact remains that it is more interesting to study the evolution of the sunshine intensity from sunrise to sunset, considering different estimations of inclination and azimuth angles for a tilted surface. Eminent researchers and authors have studied the inclination effects of the sensor's receiving surface on the global daily radiation collected and its relationship with the local latitude L (Duffie and Beckman 2013; Goswami 2015). They have explained how to get the optimum tilt angle that captures the maximum energy and recommend the following optimal slope angles: β_{opt} = L + 15° for winter periods, β_{opt} = L – 15° for summers, and a fixed value of β_{opt} = L for yearly use. However, it was found that a deviation of 15° from the optimum produced a decrease in the captured solar energy of about 5%.

Researchers are working to improve the performance of the thermal efficiency and outlet temperature of the solar thermal processes. Mzad et al. have scrutinized, experimentally and numerically, double-glazed solar collectors tested in different locations in Algeria using

the Collares-Pereira and Erbs models. The thermal parameters of the studied sensor in the north–western country, such as the variation of fluid temperature and the panel efficiency, were calculated using only the measured global-horizontal radiation (Mzad 2008). The solar air collector investigated in the north–east part of the country allowed the determination of the useful energy and the efficiency using a tilt and orientation optimization (Mzad et al. 2018). A trial solar air heater (SAH) was constructed and subjected to performance testing (Mzad, Bey, and Khelif 2019). The designed panel was able to procure an efficiency of 50% almost all year for an air flow rate of 52 $m^3/h/m^2$, and a useful energy of around 4500 W. The thermal performance simulation achieved allowed the estimation of daily solar radiation, useful power, and collector efficiency.

A novel SAH design with long-term heating, especially during off-sunny hours, was found to deliver high thermal efficiencies of up to 80% with forced convection (Saxena, Srivastava, and Tirth 2015). A mixture of desert and granular carbon has been used as thermal heat storage inside the SAH, and two halogen lights were placed in the inlet and outlet ducts.

Experimental and numerical investigations into the effect of porous metal foam on the performance of a flat-plate solar collector have been carried out (Saedodin et al. 2017). The numerical results show that the maximum thermal performance is obtained in a porous layer with a dimensionless thickness greater than 0.8. In the experimental section, the effects of metal foam on the solar collector performance at different flow rates were examined. Numerical and experimental results have shown that using the porous medium enhances the maximum thermal efficiency and Nusselt number.

Mahmood (2020) invented a new SAH design using a double-pass unglazed transpired collector. The absorbing area was increased by using wire mesh layers, and the thermal performance was enhanced by using a perforated absorber plate and a double-pass counter-flow collector in the duct.

A mathematical model was used to estimate the total solar radiation on the tilted PV surface and to determine the optimum tilt angles for a PV panel installed in Sanliurfa, Turkey (Kacira et al. 2004). The optimum tilt angles were determined using fixed and solar tracking panels. This study concluded that the monthly optimum tilt angle changes throughout the year, with a minimum value of 13° in June and a maximum value of 61° in December.

Based on an isotropic radiation model of the sky, the numerical approach proposed by Li and Lam (2007) allows predicting the solar radiation on inclined surfaces of different orientations using the measured sky radiances in the city of Hong Kong. They found that the maximum value of the tilt angle was 30° when the azimuth angle of the surface was 210°.

Jamil Ahmad and Tiwari (2009) have optimized the tilting of solar flat-plate collectors facing toward the equator using New Delhi as a reference. The calculations were based upon the measured values of the monthly mean of global and diffuse solar radiation on a horizontal surface. The annual optimum tilt angle was found to be approximately equal to the latitude of the location, and the loss in the amount of collected energy was only around 1% if the angle of tilt is adjusted seasonally.

The possibility of reducing the number of solar cooling panels based on evacuated tubes producing hot water at a low temperature (90 °C) and a water-ammonia absorption chiller was demonstrated by Corrada et al. (2014) in the South–East Queensland region. Calculations using the Liu and Jordan model suggest that the flat panel configuration is the best solution for a solar cooling and heating system, considering the cost involved in the installation and maintenance of a variable angle system.

Elminir et al. (2006) have investigated the optimum tilt and orientation angles for solar flat-plate collectors used in Helwan, Egypt. They have performed a statistical comparison of three specific anisotropic models (Tamps-Coulson, Perez, and Bugler) to use the one that provides the most accurate estimation of the total solar radiation. The study revealed that the Perez model shows the best overall calculated performance.

A simple mathematical procedure for the estimation of the optimal tilt angle of a collector was presented based on the monthly horizontal radiation (Tang and Wu 2004). The optimal tilt angle of the south-facing collectors was outlined based on the monthly horizontal radiation of 152 places around China, except for places with a considerably lower clearness index. The optimal tilt angle of other 30 cities was determined based on the actual monthly diffuse radiation.

Handoyo, Ichsani, and Prabowo (2013) have obtained an equation delivering the optimal angle of a solar collector installed in Surabaya, Indonesia. The result was compared to the work of Tang et al. and Duffie and Beckman's equations, and confirmed the validity of the equation to obtain the optimal tilt angle. They have also proposed a two-collector configuration, one facing east to be used in the morning and one facing west in the afternoon. The optimal tilt angle for these orientations was located between 36° and 39.4°.

An optimization study of the positioning of a solar energy receiver to improve the energetic gain with the Liu-

Jordan isothropic mathematical model has been carried out (Frydrychowicz-Jastrzębska 2011). The influence of the reflectivity coefficient of the ground and the transparency coefficient of the atmosphere on the investigated angle has been taken into account. The simulation revealed that 32° was the optimum angle, independently of the season, for the city of Warsaw.

Kambezidis and Psiloglou (2021) have demonstrated a new way of defining the optimal tilt angle of a solar collector in Greece that faces south. This methodology has also been implemented for finding the optimum tilt angle of flat-plate solar panels in Saudi Arabia for fixed-tilt to the south, fixed-tilt tracking the Sun, and variable-tilt tracking the Sun configurations (Farahat et al. 2021a, 2021b, 2022; Kambezidis et al. 2021). In both countries, certain constant tilt angles were determined all over the year for the first and second configuration modes.

A solar collector's efficiency will increase when it is always facing the sun, which means a tracking system is required. A tracking system is too expensive for people who live in the hills of the city of Annaba, our case study. In this paper, the estimation of optimal angles (surface tilt and azimuth) is obtained by solving the daily integration model of Gueymard (2000) and three interlinked optimization models. Fundamental solar radiation equations were programmed, using a Matlab code, to determine optimum angles via maximizing the angle of incidence of beam radiation on the collector. Obtained graphs, generating average monthly radiation, are analyzed to investigate solar radiation at some tilt angles. The results are then compared to two experimental studies in order to determine suitable periodic optimum tilt angles for solar collectors at the current latitude. The performed simulation allows a limited number of intervals per year for panel setting. The user does not need to change the collector position every month.

Site information and solar radiation modeling

Site's data

Based on the meteorological data available for the site of Annaba city in 2018, we apply the Gueymard model in order to graphically estimate the appropriate angles of solar panels. The city of Annaba is located in the northeast of Algeria in the Mediterranean Sea, 600 km from the capital, Algiers, and close to the Tunisian border. The place's geographical coordinates are:

L = 36°54′47″ North and l_{local} = 07°43′54″ East.

Klein (1977) proposed the mean day of the month, which is a date where the declination is closest to the mean declination of that month (Table 1). Using the mean day of each month can lead to small errors in the monthly extraterrestrial radiation mean value $\overline{H}_0$. The resulting values of the daily total radiation on a horizontal surface are imported from the photovoltaic geographical information system (PVGIS) for the city of Annaba.

Solar radiation on a horizontal plane

The declination is the angle between the Earth–Sun line and the equatorial plane, which is a function of the time of the year and, therefore, it varies from +23.5° on June 21 to −23.5° on December 21. This angle can be calculated with an accuracy of ±0.035° using the equation (Duffie and Beckman 2013):

$$\begin{aligned}\delta_s = {} & (180/\pi)(0.006918 - 0.399912\cos B \\ & + 0.070257\sin B - 0.006758\cos 2B \\ & + 0.000907\sin 2B - 0.002697\cos 3B \\ & + 0.00148\sin 3B)\end{aligned} \quad (1)$$

With,

$$B = (n-1)\frac{360}{365} \quad (2)$$

n is the year's day number ($1 \le n \le 365$).

The sunset/sunrise angle depends on the declination angle and is defined as:

$$\omega_{ss} = -\cos\omega_{sr} = \cos^{-1}(-\tan L \ \tan\delta_s) \quad (3)$$

And the day length is calculated as:

$$S_0 = \frac{2}{15}\ \omega_{ss} \quad (4)$$

The sun's position is marked by two important angles, the zenith and the azimuth. According to Duffie and Beckman (2013), the zenithal angle of the sun is calculated by the equation:

$$\theta_z = a\cos(\cos L \ \cos\delta_s \ \cos\omega + \sin L \ \sin\delta_s) \quad (5)$$

where the hourly angle of the sun can be written as:

Table 1: Daily-average global radiation on a horizontal surface, 2018 (PVGIS database website 2018).

Month	Jan.	Feb.	Mar.	Apr.	May	Jun.	Jul.	Aug.	Sep.	Oct.	Nov.	Dec.
Mean day	17	16	16	15	15	11	17	16	15	15	14	10
Day of the year	17	47	75	105	135	162	198	228	258	288	318	344
H_h, [kW/m^2]	1.841	3.121	4.570	6.991	7.909	7.002	8.113	6.671	4.638	4.484	2.822	2.798

$$\omega = (ST - 12) \quad 15° \tag{6}$$

The solar time equation is:

$$ST = LST + \frac{ET}{60} + \frac{1}{15} \quad (l_{st} - l_{local}) \tag{7}$$

where the equation of time is given by:

$$\begin{aligned} ET = {} & 229.18\,(0.000075 + 0.001868 \cos B \\ & - 0.032077 \sin B - 0.014615 \cos 2B \\ & - 0.04089 \sin 2B) \end{aligned} \tag{8}$$

The solar azimuth angle is the angle formed by the sun's rays in the horizontal plane with respect to the south:

$$a_s = \text{sign}(\omega)\left|\cos^{-1}\left(\frac{\cos(90 - \alpha)\sin L - \sin \delta_s}{\sin(90 - \alpha)\cos L}\right)\right| \tag{9}$$

Extraterrestrial solar radiation is the power of the sun to a horizontal surface at the top of the Earth's atmosphere, expressed as follows (Kalogirou 2014):

$$H_0 = kG_{sc}R\left[\cos L \cos \delta_s \sin \omega_{ss} + \frac{\pi\omega_{ss}}{180}\sin L \sin \delta_s\right] \tag{10}$$

Where $k = 24/\pi$ and $G_{SC} = 1.3661$ kW/m^2, the new measured solar constant value (Goswami 2015).

R is the correction factor of the sun–earth distance. According to Goswami (2015), the expression of R is:

$$\begin{aligned} R = {} & \left(\frac{D_0}{D}\right)^2 \\ & = 1.000110 + 0.034221 \cos B + 0.001280 \sin B \\ & \quad + 0.000719 \cos 2B + 0.000077 \sin 2B \end{aligned} \tag{11}$$

The clearness index, for the month "m", represents the ratio of solar radiation that penetrates the atmosphere to extraterrestrial irradiation:

$$K_t(m) = \frac{H_h(m)}{H_0} \tag{12}$$

Where $H_h(m)$ is the daily total solar radiation on a horizontal surface, which values are mentioned in Table 1.

The average daily diffuse radiation on a horizontal surface is given by the following De Miguel et al. (2001) correlation, well suited to the region enclosing the Mediterranean Sea:

$$\frac{H_d}{H_h} = 0.952 \quad \text{for } K_t \le 0.13 \tag{13}$$

$$\frac{H_d}{H_h} = 0.868 + 1.335\,K_t - 5.782\,K_t^2 + 3.721\,K_t^3 \quad \text{for } 0.13 < K_t \le 0.80 \tag{14}$$

$$\frac{H_d}{H_h} = 0.141 \text{ for } K_t > 0.80 \tag{15}$$

The daily direct radiation on the horizontal plane is merely deduced by:

$$H_{b,h} = H_h - H_d \tag{16}$$

The Gueymard DI model

The approach consists of superimposing graph curves of solar radiation falling on the panel surface at a fixed orientation with those at different tilts. So, this procedure is repeated each time the orientation of the sensor changes to obtain a group of four figures every single month. This graphical optimization method is based on a number of parameters like the average daily radiation value of the studied location, which includes the typical day and the appropriate diffuse radiation model for the situation.

The Gueymard coefficients are described as follows:

$$q = \cos L \quad \cos \delta_s \tag{17}$$

$$A(\omega_{ss}) = \sin \omega_{ss} - \frac{\pi\omega_{ss}}{180}\cos \omega_{ss} \tag{18}$$

$$\sin h_0 = q\frac{A(\omega_{ss})}{\omega_{ss}} \tag{19}$$

h_0 is an angle expressing the daily average solar elevation outside the atmosphere.

$$B(\omega_{ss}) = \omega_{ss}\frac{\pi}{180}\left(0.5 + \cos^2\omega_{ss}\right) - 0.75\sin 2\omega_{ss} \tag{20}$$

And the relationship of hourly and daily diffuse radiations on a horizontal surface, given by Liu and Jordan:

$$I_d = r_d H_d \tag{21}$$

Where the ratio of hourly diffuse to daily diffuse radiation is defined as follows:

$$r_d = \frac{\pi}{24}\frac{\cos\omega - \cos\omega_{ss}}{A(\omega_{ss})} \tag{22}$$

The relationship between the ratio of hourly to daily diffuse radiation and the ratio of hourly to daily total radiation established by Gueymard is:

$$\begin{aligned} r_t = r_d[1 + q(a_1/a_2)kA(\omega_{ss})r_d] \\ /[1 + q(a_1/a_2)B(\omega_{ss})/A(\omega_{ss})] \end{aligned} \tag{23}$$

Taking into account the atmospheric extinction effect, Gueymard (Gueymard 2000) introduced two coefficients, a_1 and a_2:

$$a_1 = 0.41341K_t + 0.61197K_t^2 - 0.01886K_tS_0 + 0.00759S_0 \tag{24}$$

$$a_2 = \mathrm{Max}\begin{bmatrix} 0.054, \\ 0.28116 + 2.2475K_t - 1.76118K_t^2 - 1.84535\sin h_0 + 1.6811\sin^3 h_0 \end{bmatrix} \tag{25}$$

The hourly global radiation on a horizontal surface is merely computed by:

$$I_h = r_tH_h \tag{26}$$

The hourly direct solar radiation on a horizontal surface is defined by the equation:

$$I_{b,h} = r_tH_h - r_dH_d \tag{27}$$

The hourly beam radiation on a tilted surface is calculated as:

$$\begin{aligned} I_{b,T} = R_bI_{b,h} = I_{b,h}\frac{\cos i}{\cos\theta_z} \\ = \frac{\sin\theta_z\cos(a_s - a_w)\sin\beta + \cos\theta_z\cos\beta}{\cos L\cos\delta_s\cos\omega + \sin L\sin\delta_s} \end{aligned} \tag{28}$$

i is the incident angle of the beam solar radiation on an inclined surface, given by the equation:

$$\cos i = \sin\theta_z\cos(a_s - a_w)\sin\beta + \cos\theta_z\cos\beta \tag{29}$$

Models of radiation on a sloped surface

In order to perform the calculation of the global radiation gathered by a tilted collector at various angles and azimuth orientations, an isotropic and two anisotropic sky models were implemented in a Matlab code to obtain the maximum solar intensity and determine the corresponding angles in a comparative investigation.

The Liu and Jordan isotropic sky model

Assuming an isotropic sky, the Liu and Jordan model was used:

$$I_T = I_{b,h}\frac{\cos i}{\cos\theta_z} + I_d\cos^2\frac{\beta}{2} + \rho I_h\sin^2\frac{\beta}{2} \tag{30}$$

Anisotropic sky model

Some improved models for tilted surfaces take into account the circumsolar and horizon brightness radiation components. In this study, we employed two well-known models: the Perez model and the model of Hay, Davies, Klucher, and Reindl (HDKR). These models allow for evaluation of the global radiation on a sloping plane based on the Gueymard (2000) model for predicting the solar intensity on a horizontal surface. Indeed, according to Duffie and Beckman (2013) and Yadav and Chandel (2013), it is mentioned that the HDKR model delivers predictions approaching the measured values.

Perez et al. (1990) have developed a model based on detailed analysis, which takes into account the three diffuse components. So, the diffuse radiation on a sloped surface is expressed by:

$$I_{d,T} = I_d\left[(1 - F_1)\left(\frac{1 + \cos\beta}{2}\right) + F_1\frac{a}{b} + F_2\sin\beta\right] \tag{31}$$

where F_1 and F_2 are the circumsolar and horizon brightness coefficients, respectively.

The terms a and b account for the angles of incidence of the cone of circumsolar radiation, which are given by:

$$a = \max(0, \cos(i)) \text{ and } b = \max(\cos 85, \cos(\theta_z)) \tag{32}$$

To compute the values of F_1 and F_2, first we need to calculate two parameters that describe the sky conditions: the clearness ε and the brightness Δ. The value of the clearness parameter allows us to select the Perez coefficients f_{11} to f_{23} from Table 2.

$$\epsilon = \left(\left(\frac{I_d + I_{b,N}}{I_d}\right) + 5.535\times10^{-6}\theta_z^3\right)\Big/\left(1 + 5.535\times10^{-6}\theta_z^3\right) \tag{33}$$

Table 2: Coefficients of the Perez model.

Range of ε	f_{11}	f_{12}	f_{13}	f_{21}	f_{22}	f_{23}
1.000–1.065	−0.008	0.588	−0.062	−0.060	0.072	−0.022
1.065–1.230	0.130	0.683	−0.151	−0.019	0.066	−0.029
1.230–1.500	0.330	0.487	−0.221	0.055	−0.064	−0.026
1.500–1.950	0.568	0.187	−0.295	0.109	−0.152	0.014
1.950–2.800	0.873	−0.392	−0.362	0.226	−0.462	0.001
2.800–4500	1.132	−1.237	−0.412	0.288	−0.823	0.056
4.500–6.200	1.060	−1.600	−0.359	0.264	−1.127	0.131
6.200–∞	0.678	−0.327	−0.250	0.156	−1.377	0.251

$$\text{where } I_{b,N} = I_{b,h}/\cos\theta_z \tag{34}$$

Brightness coefficients for Perez's anisotropic sky (Perez et al. 1990)

$$\Delta = m_{\text{air}}\,\frac{I_d}{I_{0N}} \tag{35}$$

$$\text{where } m_{\text{air}} = \frac{1}{\cos\theta_z} \text{ and } I_{0N} = G_{sc}R \tag{36}$$

$$F_1 = \max\left[0, \left(f_{11} + f_{22}\,\Delta + \frac{\pi\,\theta_z}{180} f_{13}\right)\right];\ F_2 = f_{21} + f_{22}\,\Delta + \frac{\pi\,\theta_z}{180} f_{23} \tag{37}$$

$$\text{It comes to : } I_T = R_b I_{b,h} + I_{d,T} + I_h \rho\left(\frac{1-\cos\beta}{2}\right) \tag{38}$$

The HDKR model (Reindl, Beckman, and Duffie 1990) is more appropriate to predict global radiation on tilted surfaces towards the equator and yields results close to the measured values. According to the authors, the diffuse radiation is defined as follows:

$$I_{d,T} = \left\{(1-A_i)\left(\frac{(1+\cos\beta)}{2}\right)\left(1 + f\sin^3\frac{\beta}{2}\right) + A_i R_b\right\} \tag{39}$$

$$\text{where } A_i = \frac{I_{b,h}}{I_0} \text{ and } f = \sqrt{I_{b,h}/I_h} \tag{40}$$

$$I_0 = G_{sc}\,R\,(\cos L\cos\delta_s\cos\omega + \sin L\sin\delta_s) \tag{41}$$

$$R_b = \frac{\cos i}{\sin\alpha} \tag{42}$$

$$\text{Hence : } I_T = R_b\,I_{b,h} + I_{d,T} + I_h\,\rho\left(\frac{1-\cos\beta}{2}\right) \tag{43}$$

Simulation and explanation of the results

The equations of the above-presented models have been computed under the Matlab code; curves are plotted giving the hourly irradiation intensity (I_T) considering the monthly mean days (Table 1) of the year 2018.

Liu and Jordan model outcomes

The curves related to a unique azimuth angle and different inclinations of the solar collector are drawn in a single figure. Consequently, for each month, a group of four graphs is obtained according to the tested values (0°/22.5°/45°/67.5°) of the surface azimuth angle. Each figure contains seven curves of hourly solar intensities in relation with the chosen tilt angles (10°/15°/20°/25°/30°/35°/40°).

The simulation carried out in the city of Annaba for the whole year 2018, using the Gueymard daily integration (DI) model, allowed us to observe peaks of instantaneous radiation between noon and 2 PM. From the first group of curves, as illustrated by Figure 1, we note that the maximum radiation recorded in January is 370 W/m^2. An inclination of 40° and an azimuthal surface angle (a_w) equal to zero correspond to this case. These slope and orientation angles (40°, 0°) remain unchanged during February, but the maximum radiation recorded is around 590 W/m^2 and at the same time the curve peaks are decreasing (Figure 2).

In examining the results for March, the maximum predicted irradiation value is 740 W/m^2, corresponding to an orientation of 0° when the solar collector is tilted at 35° (Figure 3). For the other surface azimuth angles, there is a slight decrease in the radiated flux and the curves obtained are bell-shaped. The simulation of April displays a pinnacle of 1000 W/m^2 at 12:30 PM, corresponding to an inclination of 25° and a surface azimuth angle of a_w = 0° (Figure 4). Similar results were obtained in May. Panels inclined at 20–25° and oriented toward the south are expected to emit around 1000 W/m^2 of radiation (Figure 5). Moreover, varying the panel orientation does not affect the energy collected over a wide range of tilts. Simulations of radiation during June revealed a maximum of about 860 W/m^2 at 12:30 PM, obtained when the solar collector is

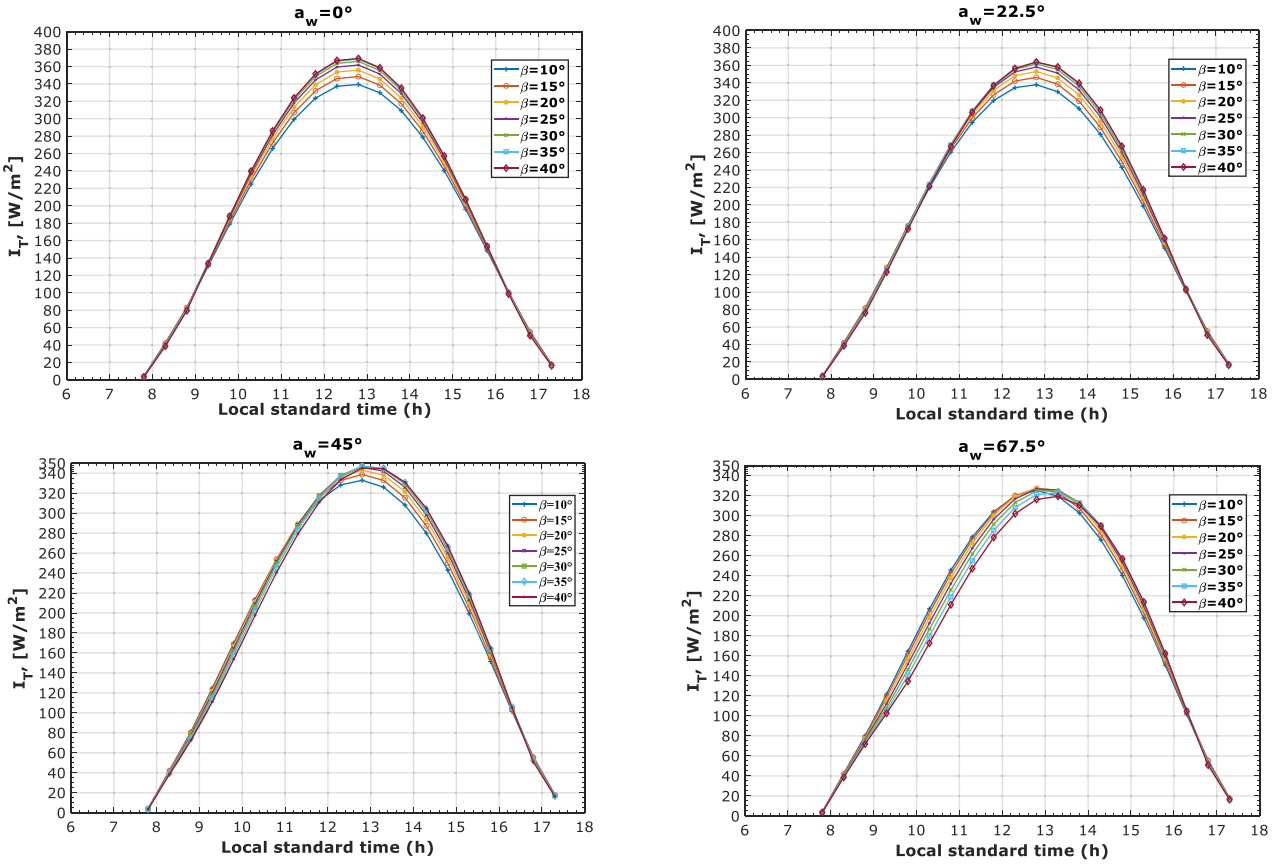

Figure 1: Monthly-average hourly global irradiation, January 17.

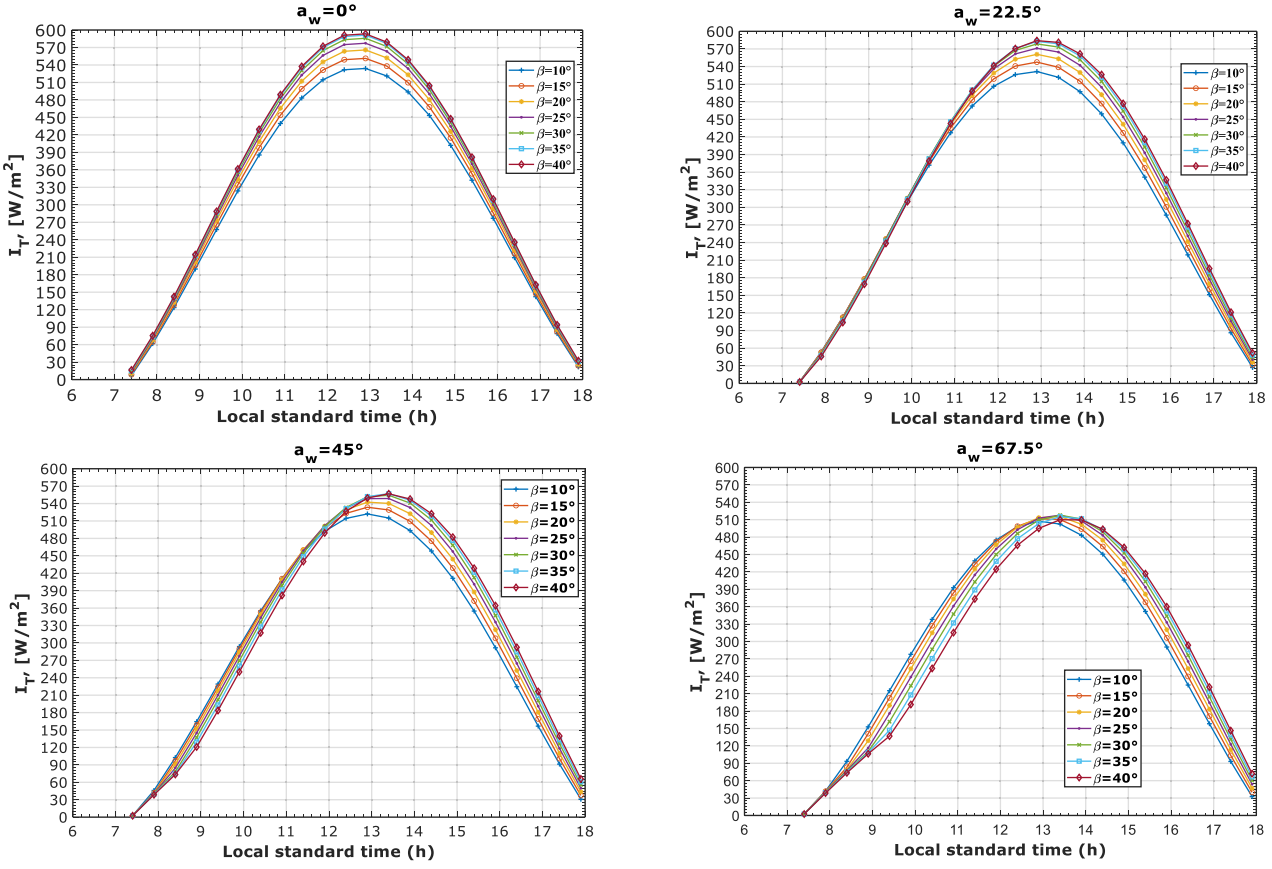

Figure 2: Monthly-average hourly global irradiation, February 16.

tilted at 10° or 15° with a south-facing surface (Figure 6). Besides, for three orientations (22.5°/45°/67.5°), predictions show the same irradiation value while the curves tend to merge and move slightly to the right, as noticed in the previous months.

In July, the maximum radiation reaches 1020 W/m^2 for a surface inclined at 15° and oriented toward the south. The curves have the same behavior as the previous ones, but they overlap in the afternoon when a_w = 22.5° (Figure 7). It should be noted that the maximum intensity value of solar radiation remains almost the same for the considered orientations. In August, the predicted incident solar radiation is approximately 900 W/m^2 when the panel is tilted 20° and oriented at a_w = 0°. For other orientations, from 22.5° to 67.5°, the intensity of the incident solar flux decreases with increasing surface azimuth angle (Figure 8).

Obviously, in September, the solar rays decrease in intensity, as evidenced by the predicted maximum value of irradiation equal to 690 W/m^2, obtained for an inclination of 30° and a full south orientation. One can note that the curves related to the angles a_w = 22.5°, 45°, and 67.5° have the same shape as the above ones (Figure 9). Higher solar incident fluxes are obtained during October, compared to September. The predictions exhibit a maximum of 860 W/m^2 for a tilted panel at 40° with full south orientation (Figure 10). However, increasing the surface azimuth angle results in a time shift of the optimal radiation curve to the right compared to the plotted curves of the first slope.

The simulation carried out for November (Figure 11) and December (Figure 12) gives maximum values of solar radiation of 645 W/m^2 and 800 W/m^2 respectively, collected on the panel inclined at 40° from the horizontal plane and oriented to the south (a_w = 0°). The illustrations representing other surface azimuth angles (22.5°, 45°, and 67.5°) show a decrease in the value of the peaks and, at the same time, a shift of the optimal curve to the right, considering the curves obtained for other inclinations.

In Table 3 we summarize the results for the inclination and orientation angles for optimal adjustment of the solar

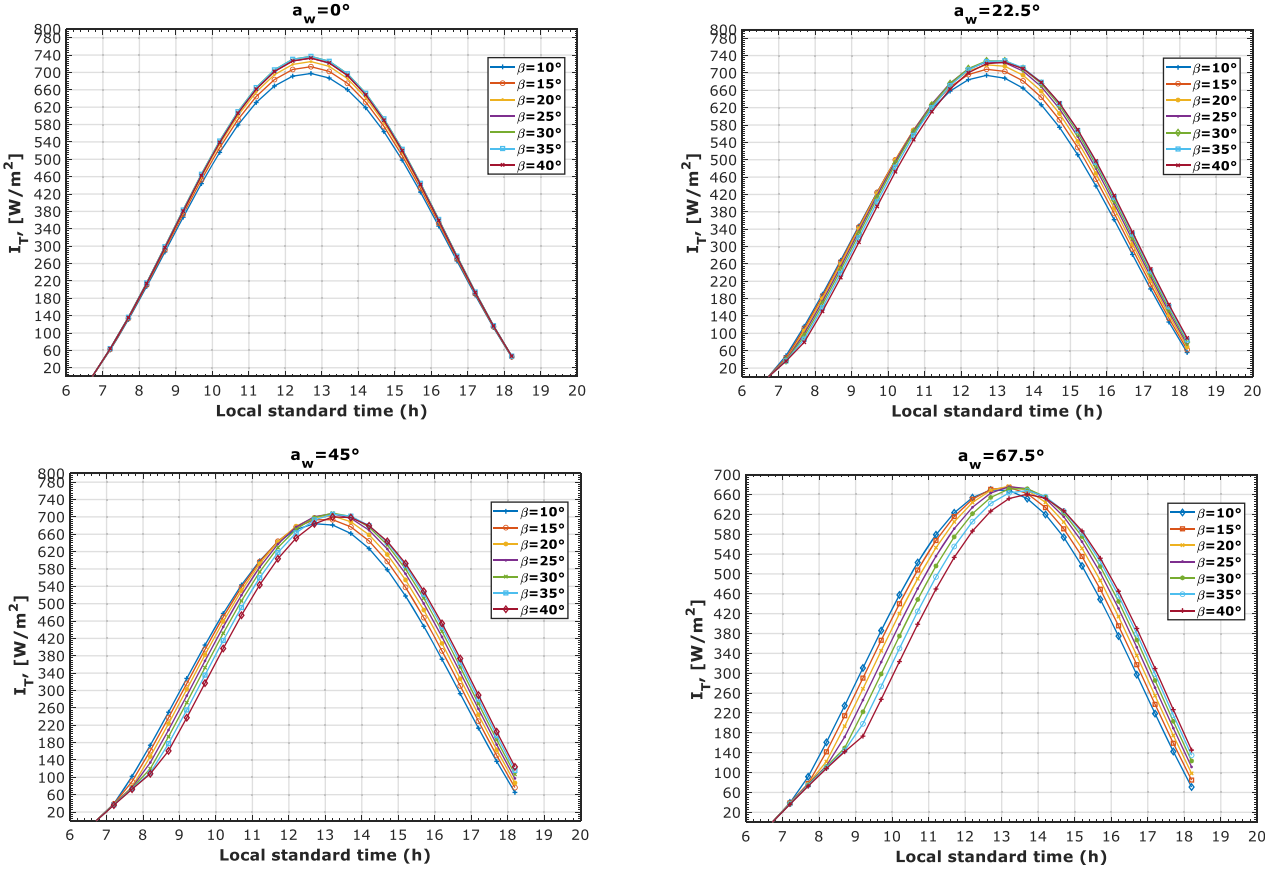

Figure 3: Monthly-average hourly global irradiation, March 16.

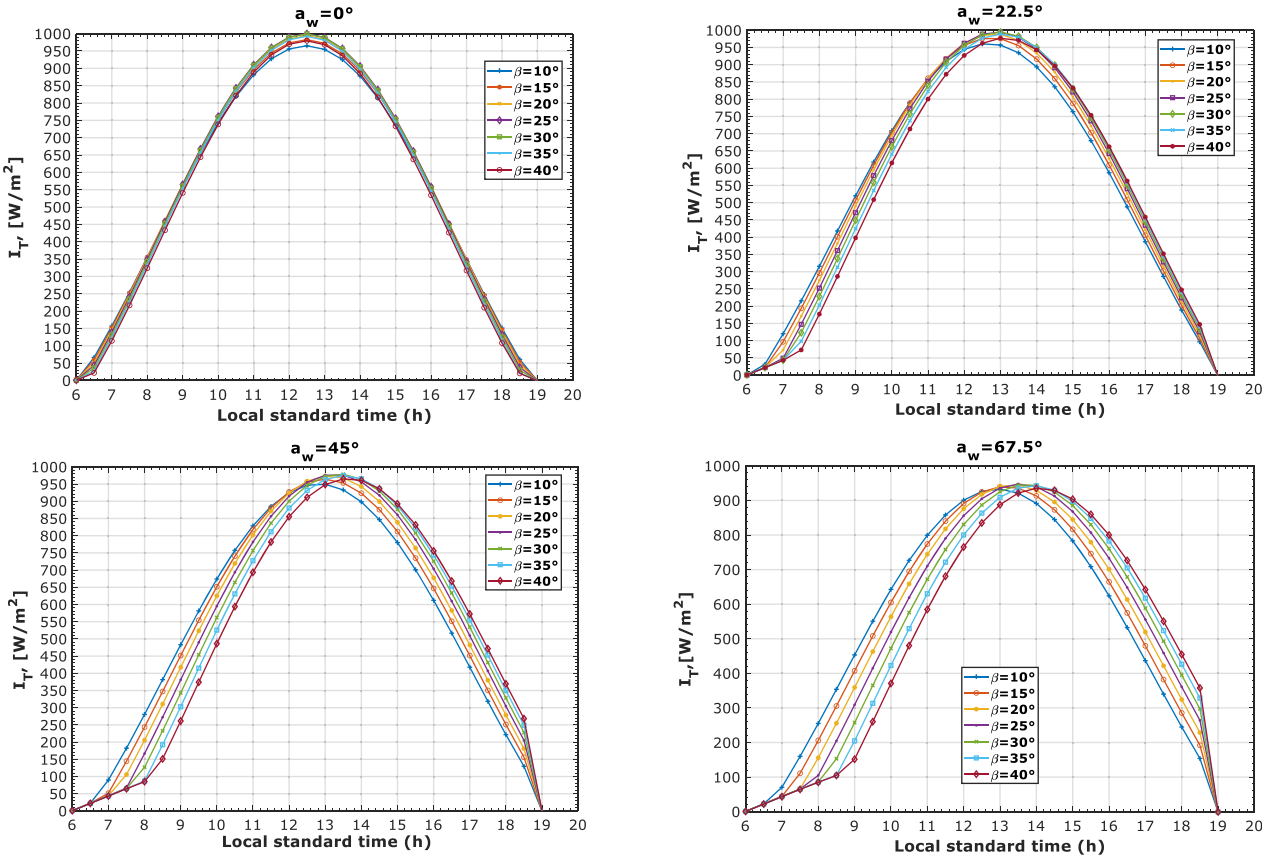

Figure 4: Monthly-average hourly global irradiation, April 15.

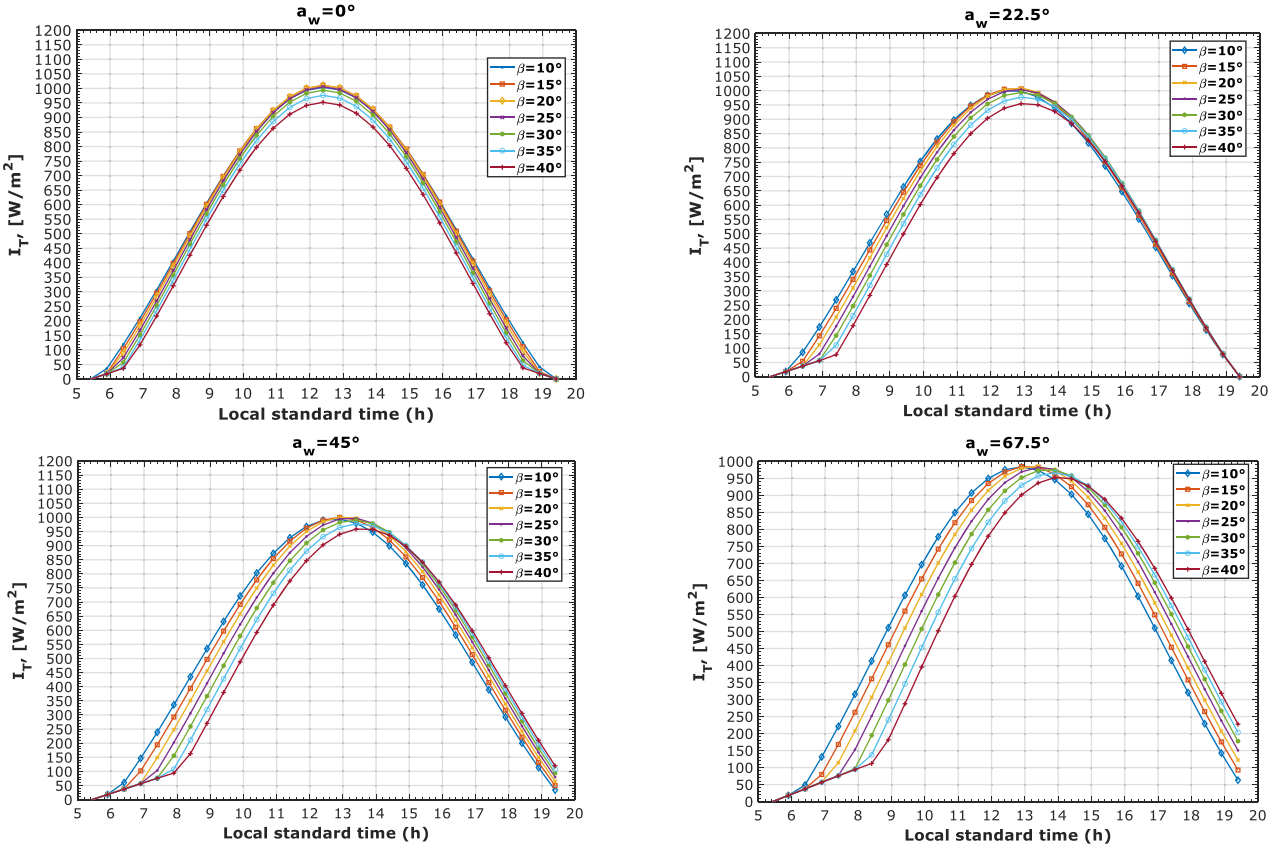

Figure 5: Monthly-average hourly global irradiation, May 15.

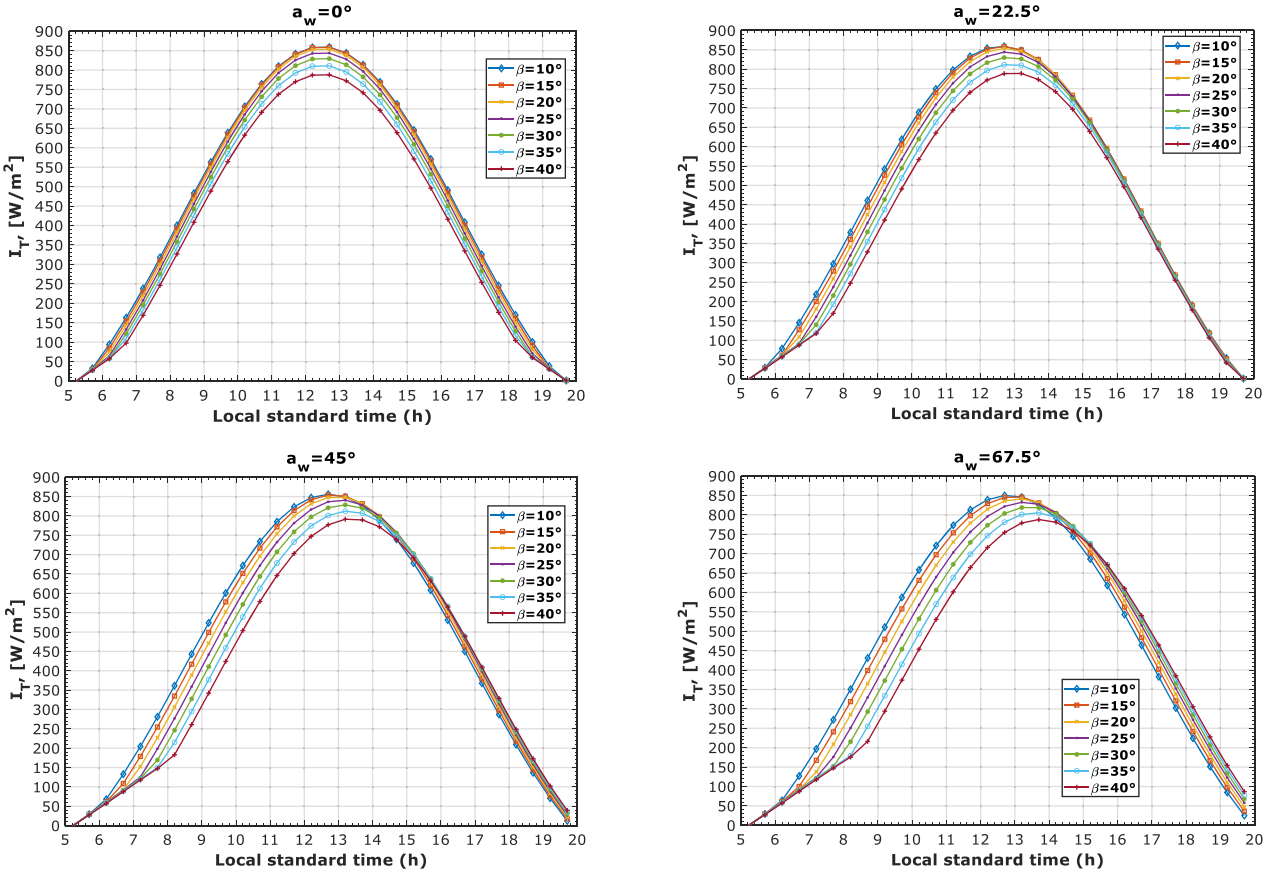

Figure 6: Monthly-average hourly global irradiation, June 11.

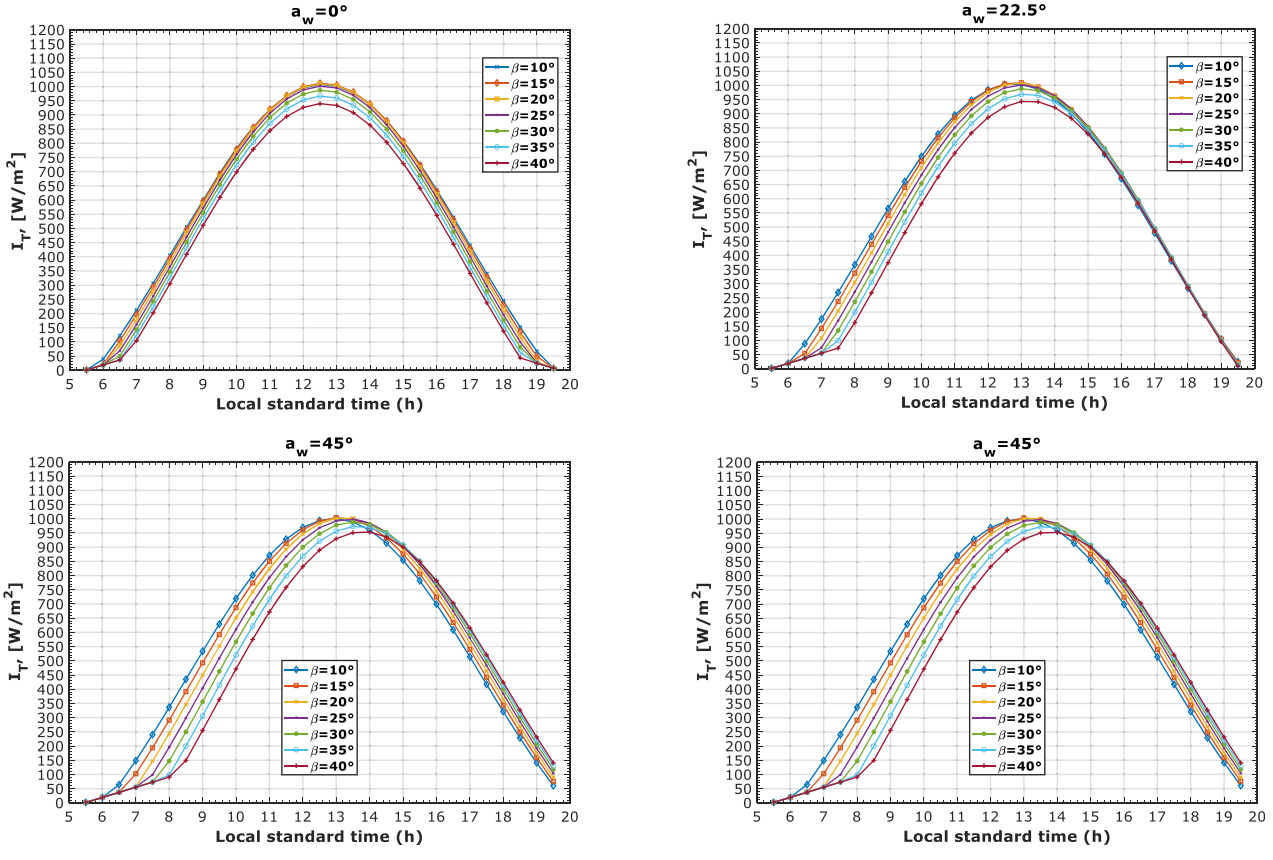

Figure 7: Monthly-average hourly global irradiation, July 17.

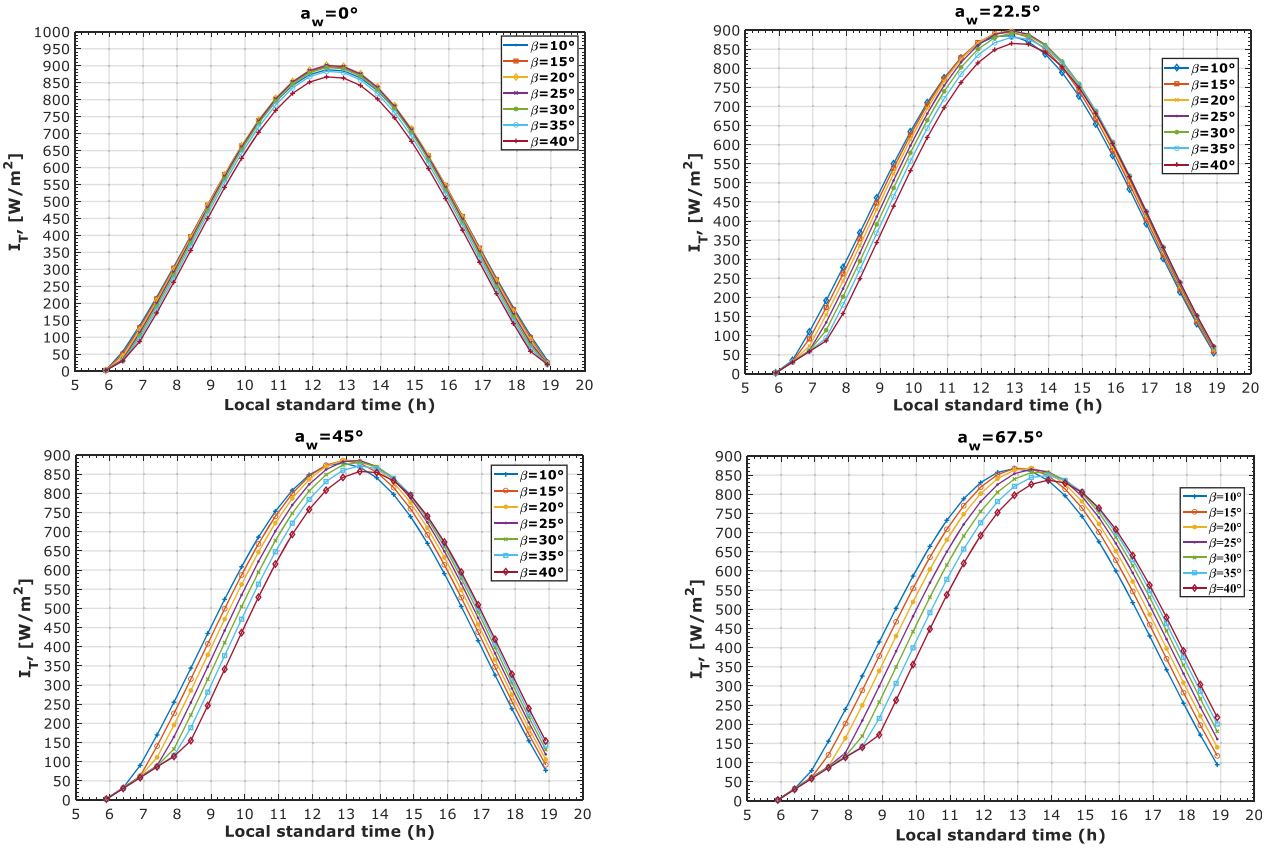

Figure 8: Monthly-average hourly global irradiation, August 16.

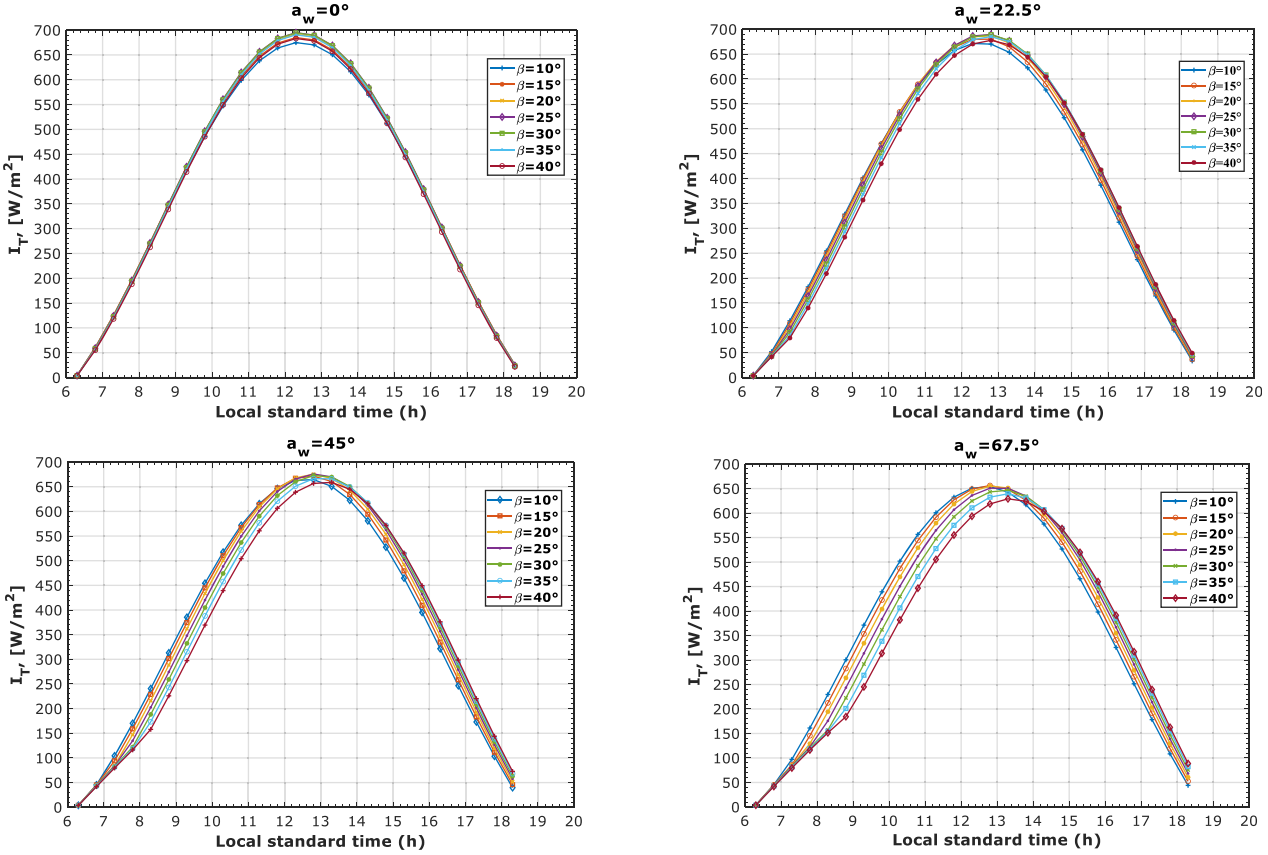

Figure 9: Monthly-average hourly global irradiation, September 15.

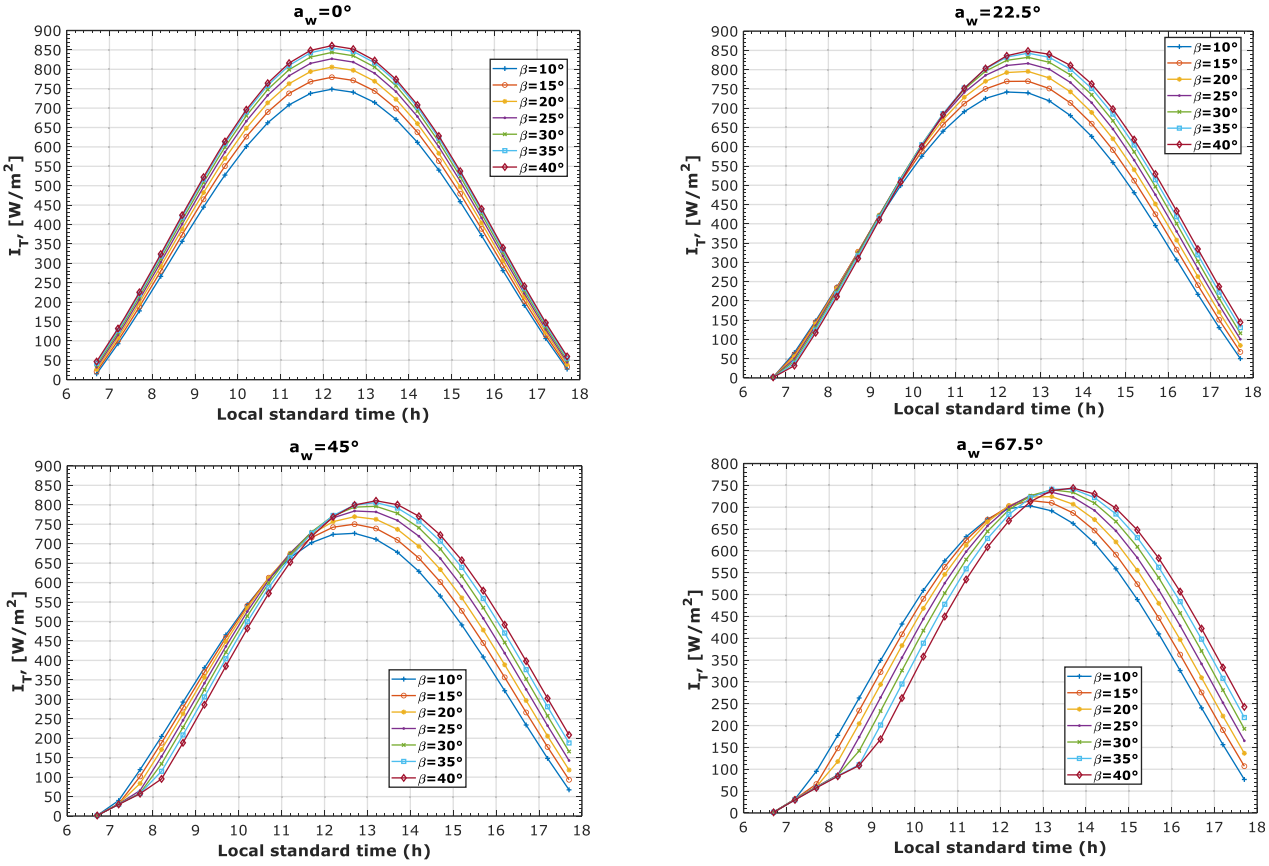

Figure 10: Monthly-average hourly global irradiation, October 15.

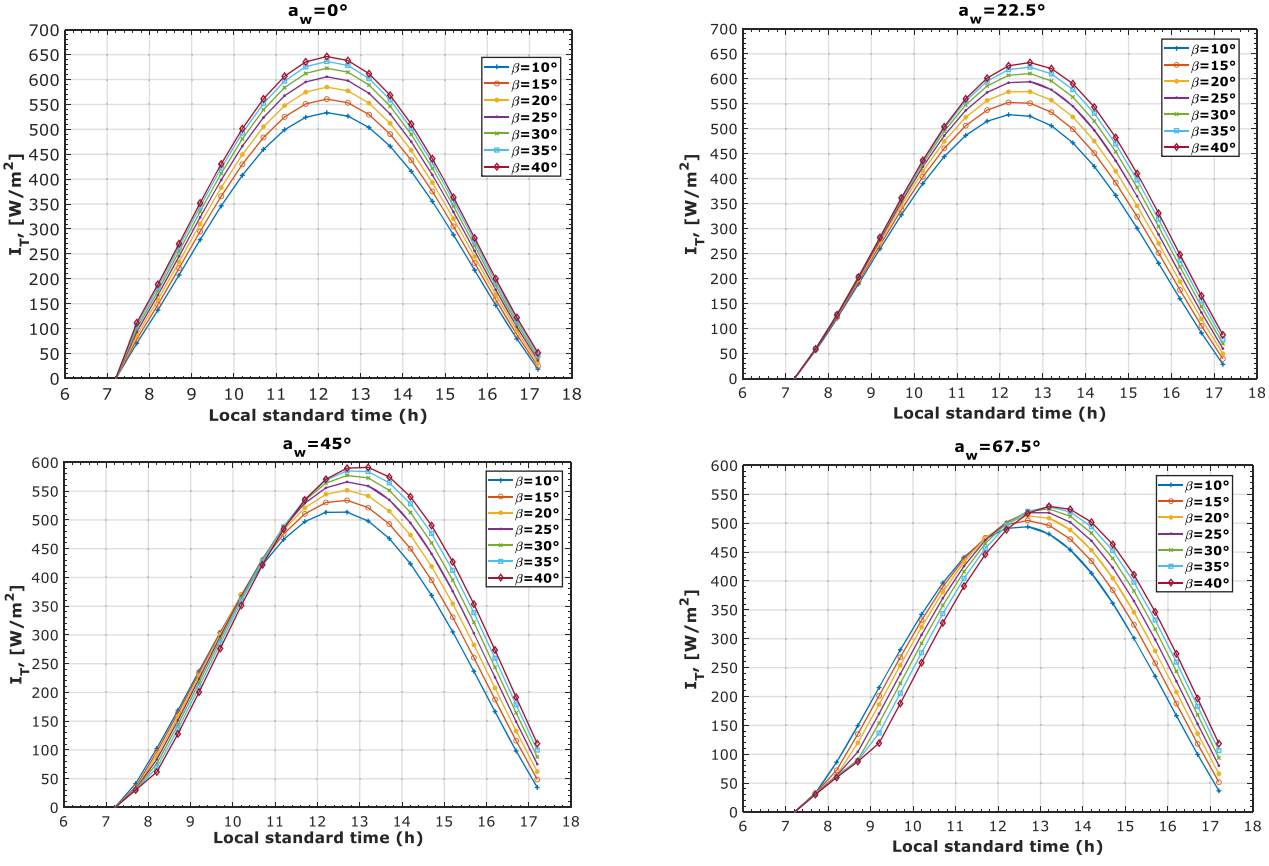

Figure 11: Monthly-average hourly global irradiation, November 14.

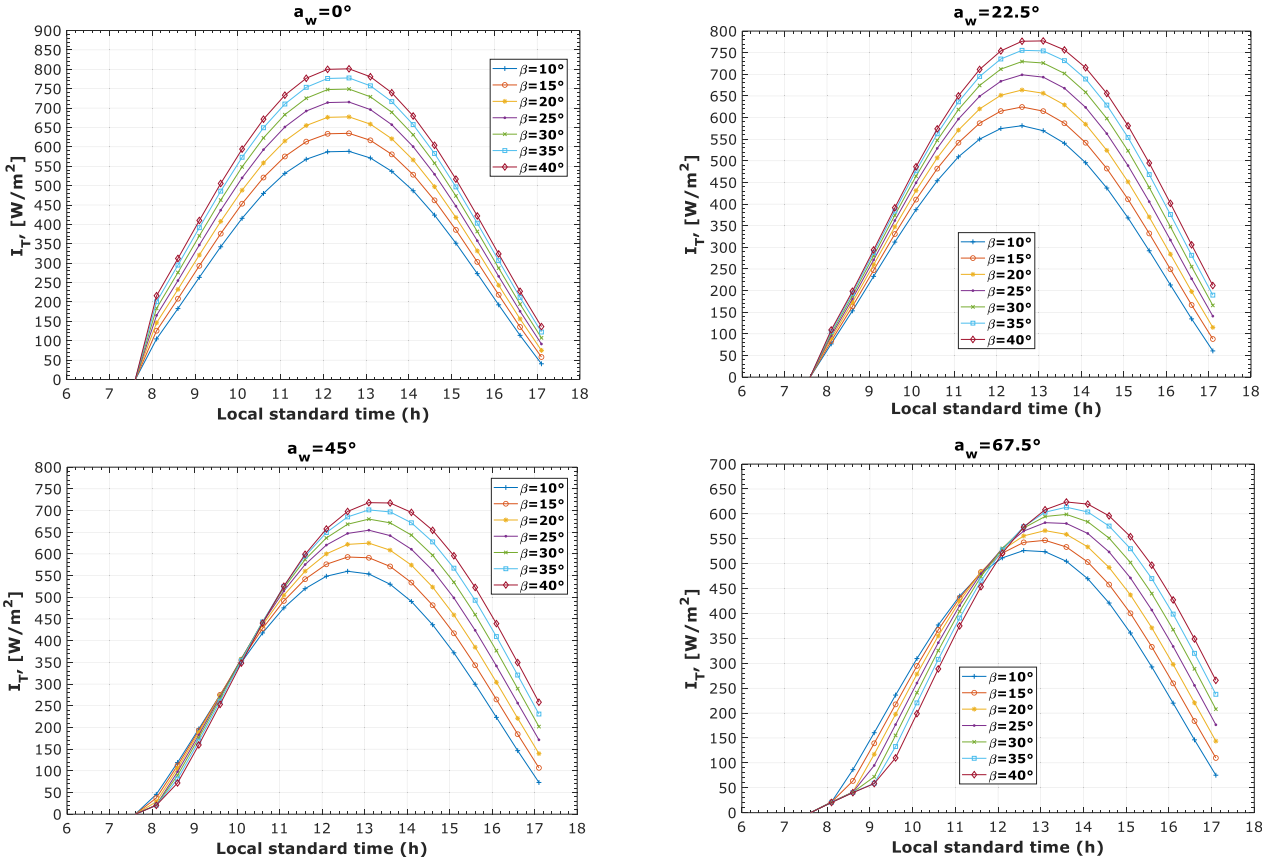

Figure 12: Monthly-average hourly global irradiation, December 10.

Table 3: Maximum irradiation and optimal angles ($a_w = 0$).

Monthly mean day	**Jan. 17**	**Feb. 16**	**Mar. 16**	**Apr. 15**	**May 15**	**Jun. 11**
Maximum solar radiation, (W/m^2)	370	590	740	1000	1010	860
Slope angle, β	40°	40°	35°	30°	10–15°	15°
Monthly mean day	**Jul. 17**	**Aug. 16**	**Sep. 15**	**Oct. 15**	**Nov. 14**	**Dec. 10**
Maximum solar radiation, (W/m^2)	1020	900	690	860	640	800
Slope angle, β	15°	25°	30°	40°	40°	40°

collector and maximum radiation corresponding to the typical days of the year 2018. It is important to point out that the predictions reveal the highest solar intensity between 12 PM and 1 PM.

HDKR and Perez models' outcomes

Concerning the simulations from the HDKR model, we chose to depict the maximum solar intensity at midday of the typical days versus tilt angle and drew curves of different azimuthal orientations for each month (Figures 13–18). The angle a_w is measured in 5° increments from –15° to 55°.

The Table below (Table 4) summarizes the results obtained in the previous simulations.

The empirical relationships of two authors were used to compare and validate the results of the present work (Table 5). El-Kassaby (1988) established correlations to determine the optimal monthly tilt angle as a function of the month. The experimental work was carried out at the University of Mu'tah (Jordan), at a latitude of L = 31°. These relationships were applied to the city of Annaba to calculate the monthly optimal angles. In addition, one of the correlations of Tiris and Tiris (1998), namely Eq. (16), was implemented in the program to estimate the optimal monthly angle in the city of Annaba.

Table 4: Maximum global radiation on optimal monthly tilts and azimuth orientations.

HDKR anisotropic												
Month	**Jan.**	**Feb.**	**Mar.**	**Apr.**	**May**	**Jun.**	**Jul.**	**Aug.**	**Sep.**	**Oct.**	**Nov.**	**Dec.**
Mean day	17	16	16	15	15	11	17	16	15	15	14	10
Max I_T, (W/m^2)	455	692	819	1028	1023	869	1020	929	759	954	763	926
β	61	57	48°	32°	22°	18°	19°	29°	45°	52°	60°	64°
a_w	5°	5°	0°	0°	0°	15°	−5°	−5°	−5°	0°	0°	5°
Perez anisotropic												
Max I_T, (W/m^2)	435	675	822	1034	1029	880	1026	944	767	955	752	909
β	52	49	42	31	22	18	19	28	37	49	57	62
a_w	5°	5°	0°	0°	0°	15°	−5°	−5°	−5°	0°	0°	5°

Table 5: A comparison of the various works' outcomes.

Month	**El-Kassaby**	**Tiris**	**This work**			
			Liu and Jordan	**Perez**	**HDKR**	**Average (Perez and HDKR)**
Jan.	64°	63°	40°	52°	61°	56.5°
Feb.	55°	54°	40°	49°	57°	53°
Mar.	40°	39°	35°	42°	48°	45°
Apr.	21°	26°	30°	31°	32°	31.5°
May	4°	12°	15°	22°	22°	22°
Jun.	0°	3°	15°	18°	18°	18°
Jul.	3°	9°	15°	19°	19°	19°
Aug.	14°	18°	25°	28°	29°	28.5°
Sep.	34°	31°	30°	37°	45°	41°
Oct.	51°	52°	40°	49°	52°	50.5°
Nov.	62°	64°	40°	57°	60°	58.5°
Dec.	66°	73°	40°	62°	64°	63°

Summary and conclusions

A simulation under a Matlab code was carried out for the performance prediction of inclined arrays in the hope of optimizing the solar collector positioning. On one hand, the Gueymard DI model associated with the simple isotropic relationship of Liu and Jordan was used. On the other hand, two more improved anisotropic models were investigated via the models of Perez and HDKR.

The graphical illustration of the results made it possible to follow the evolution of the hourly solar irradiation for the considered location and year during its daylight hours. Thanks to the wide-ranging curves, it was possible to identify the suitable inclination and orientation of the panel.

The approach considered in this case study facilitates the selection of the optimal monthly angle in each group and is more explicit in Figures 13–18. Visually, the highest curves correspond to the maximum radiation, which relates to the angles of inclination and azimuth, allowing the best performance of the solar collector. We could observe that when the surface azimuth angle increases, the curves move towards the afternoon, accompanied by a slight decrease in their peaks. This is mainly due to the direct component of the radiation on the inclined surface, which depends on the solar coordinates of the city of Annaba. Because of the term cos (a_s – a_w) in Eq. (29), significant differences between the surface and solar azimuth angles result in a decrease in radiation and a shift of the bell-shape.

The maximum predicted value of solar radiation by the present simulation was 1020–1026 W/m^2 in July for a panel tilted at 15–19°, and the minimum value was 370–455 W/m^2 in January for a panel tilted at 40–61°. We conclude that, for optimal performance, the inclination β of the solar collector must be corrected monthly with a full-south orientation (a_w = 0°), as defined in Tables 3 and 4. Furthermore, it was shown that the monthly mean hourly global radiation as a function of the monthly mean daily maximum possible number of sunshine hours is clearly dependent on latitude for high latitudes (Soler and Gopinathan 1994). This statement was evidenced by the results,

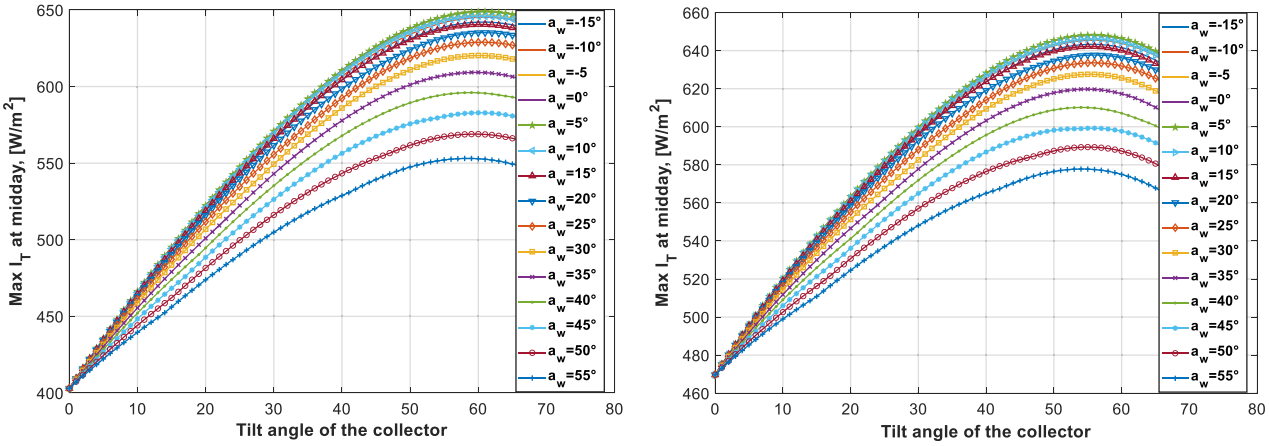

Figure 13: Maximum amounts of solar radiation (Jan. 17 and Feb. 16).

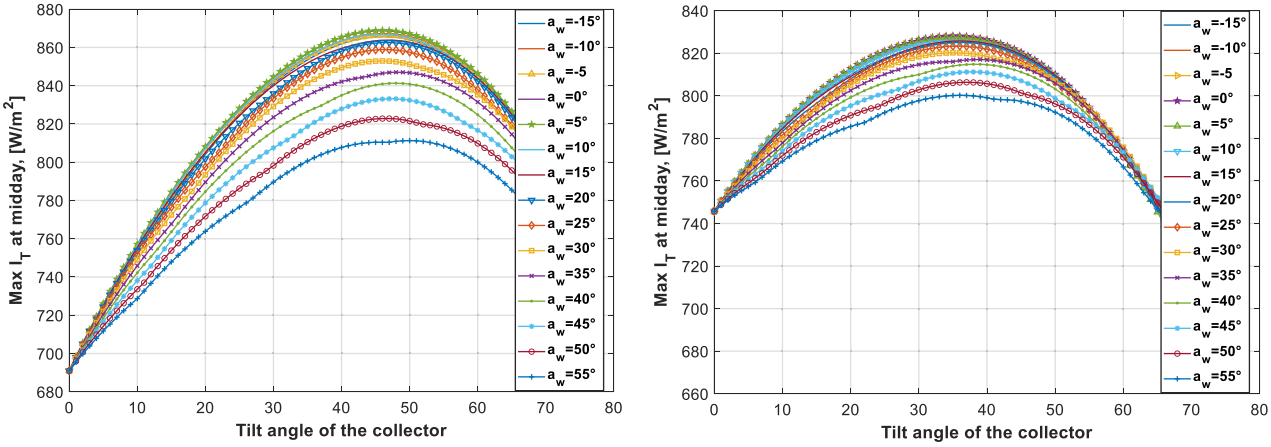

Figure 14: Maximum amounts of solar radiation (Mar. 16 and Apr. 15).

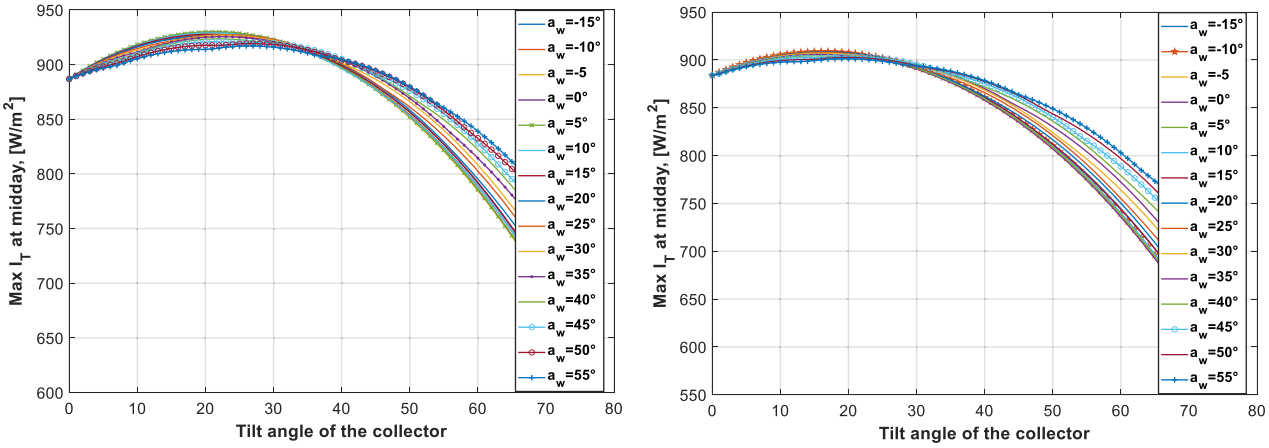

Figure 15: Maximum amounts of solar radiation (May 15 and June 11).

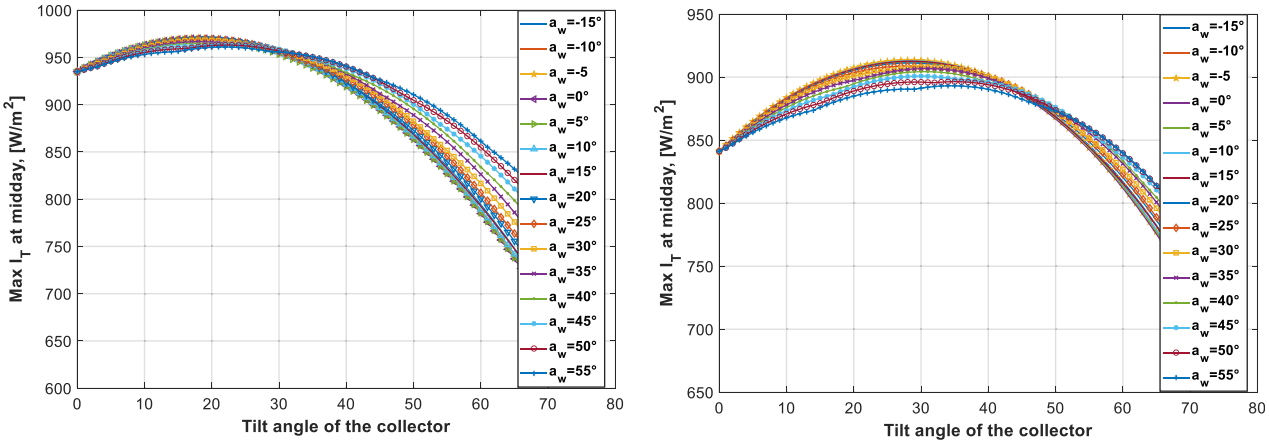

Figure 16: Maximum amounts of solar radiation (Jul. 17 and Aug. 16).

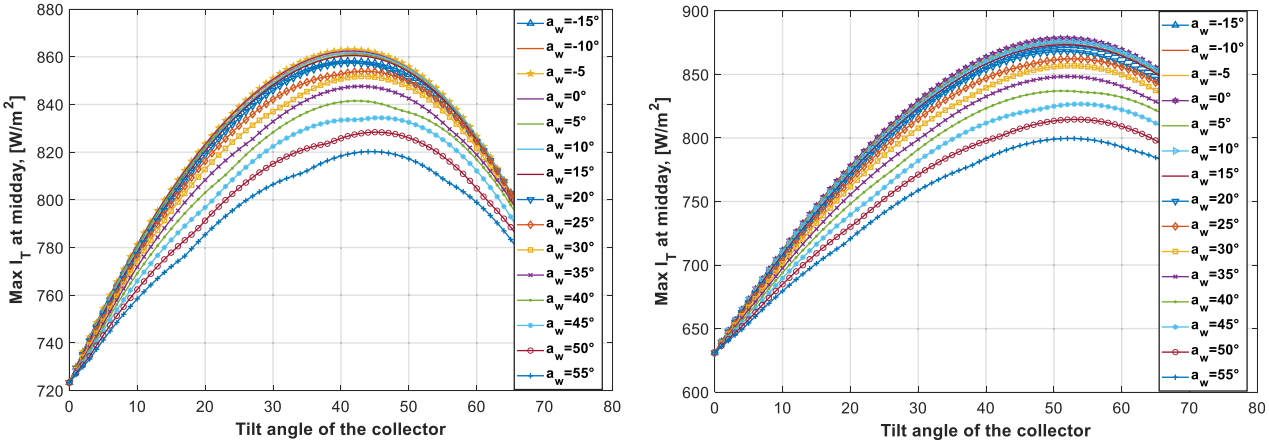

Figure 17: Maximum amounts of solar radiation (Sep. 15 and Oct. 15).

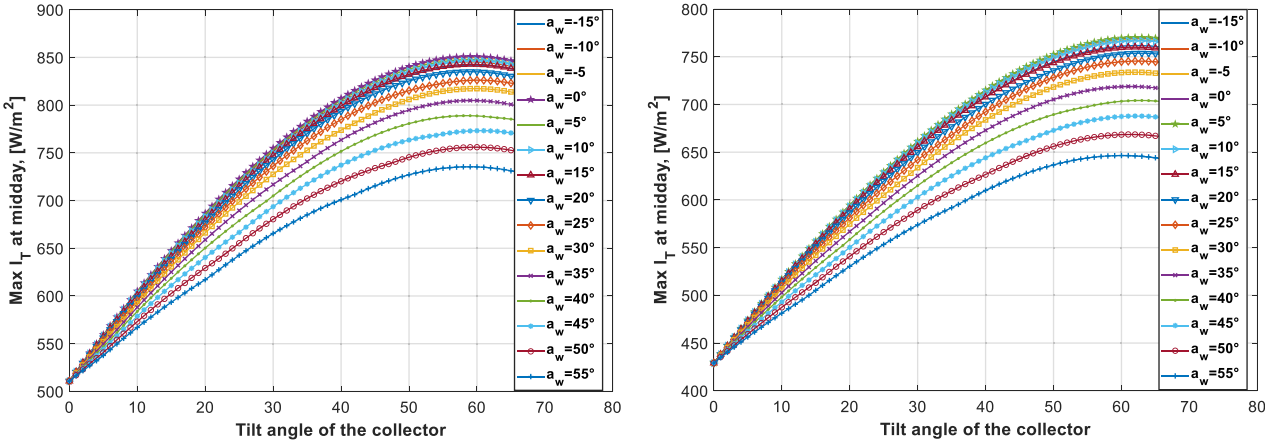

Figure 18: Maximum amounts of solar radiation (Nov. 14 and Dec. 10).

particularly in autumn (Figures 9–12) and winter (Figures 1 and 2). In fact, the latitudinal effect was taken into account in the previous relationships and thus implies the cities that have different latitudes from Annaba city.

Finally, comparing the results of the Liu and Jordan model with the average results from the Perez and HDKR models, the following recommendations are put forward for Annaba:

- $\beta = 54° (L + 17°)$ is the recommended angle for the months between October and March. The models of Perez and HDKR are the best options to maximize the radiation collected because there will be significant radiation gain (26.7%) throughout this period.
- $\beta = 26° (L - 11°)$ is the recommended angle for the months between April and September. The model of Liu and Jordan and the models of Perez and HDKR are both the best options because of regularity and having constant radiation during the considered period.

Author contributions: All the authors have accepted responsibility for the entire content of this submitted manuscript and approved submission.
Research funding: None declared.
Conflict of interest statement: The authors declare no conflicts of interest regarding this article.

References

Collares-Pereira, M., and A. Rabl. 1979. "The Average Distribution of Solar Radiation-Correlations between Diffuse and Hemispherical and between Daily and Hourly Insolation Values." *Solar Energy* 22 (2): 155–64.

Corrada, P., J. Bell, L. Guan, and N. Motta. 2014. "Optimizing Solar Collector Tilt Angle to Improve Energy Harvesting in a Solar Cooling System." *Energy Procedia* 48: 806–12.

De Miguel, A., J. Bilbao, R. Aguiar, H. Kambezidis, and E. Negro. 2001. "Diffuse Solar Irradiation Model Evaluation in the North Mediterranean Belt Area." *Solar Energy* 70 (2): 143–53.

Duffie, J. A., and W. A. Beckman. 2013. *Solar Engineering of Thermal Processes*, 4th ed. Hoboken, New Jersey: John Wiley & Sons.

El-Kassaby, M. M. 1988. "Monthly and Daily Optimum Tilt Angle for South Facing Solar Collectors; Theoretical Model, Experimental and Empirical Correlations." *Solar & Wind Technology* 5 (6): 589–96.

Elminir, H. K., A. E. Ghitas, F. El-Hussainy, R. Hamid, M. M. Beheary, and K. M. Abdel-Moneim. 2006. "Optimum Solar Flat-Plate Collector Slope: Case Study for Helwan, Egypt." *Energy Conversion and Management* 47 (5): 624–37.

Erbs, D. G., S. A. Klein, and J. A. Duffie. 1982. "Estimation of the Diffuse Radiation Fraction for Hourly, Daily and Monthly-Average Global Radiation." *Solar Energy* 28 (4): 293–302.

Farahat, A., H. D. Kambezidis, M. Almazroui, and E. Ramadan. 2021. "Solar Potential in Saudi Arabia for Southward-Inclined Flat-Plate Surfaces." *Applied Sciences* 11 (9): 4101–25.

Farahat, A., H. D. Kambezidis, M. Almazroui, and M. Al Otaibi. 2021. "Solar Potential in Saudi Arabia for Inclined Flat-Plate Surfaces of Constant Tilt Tracking the Sun." *Applied Sciences* 11 (15): 7105–29.

Farahat, A., H. D. Kambezidis, M. Almazroui, and E. Ramadan. 2022. "Solar Energy Potential on Surfaces with Various Inclination Modes in Saudi Arabia: Performance of an Isotropic and an Anisotropic Model." *Applied Sciences* 12 (11): 5356–76.

Frydrychowicz-Jastrzębska, G. 2011. "The Effect of Spatial Orientation of Solar Energy Receiver on the Energetic Gain." *Renewable Energies and Power Quality Journal* 1 (9): 484–9.

Goswami, D. Y. 2015. *Principles of Solar Engineering*, 3rd ed. Boca Raton, Florida: Taylor & Francis Group, CRC Press.

Gueymard, C. 2000. "Prediction and Performance Assessment of Mean Hourly Global Radiation." *Solar Energy* 68 (3): 285–303.

Handoyo, E. A., D. Ichsani, and Prabowo. 2013. "The Optimal Tilt Angle of a Solar Collector." *Energy Procedia* 32: 166–75.

Jamil Ahmad, M., and G. N. Tiwari. 2009. "Optimization of Tilt Angle for Solar Collector to Receive Maximum Radiation." *The Open Renewable Energy Journal* 2: 19–24.

Kacira, M., M. Simsek, Y. Babur, and S. Demirkol. 2004. "Determining Optimum Tilt Angles and Orientations of Photovoltaic Panels in Sanliurfa, Turkey." *Renewable Energy* 29 (8): 1265–75.

Kalogirou, S. A. 2014. *Solar Energy Engineering Processes and Systems*, 2nd ed. Waltham, Massachusetts: Academic Press, Elsevier.

Kambezidis, H. D., and B. E. Psiloglou. 2021. "Estimation of the Optimum Energy Received by Solar Energy Flat-Plate Convectors in Greece Using Typical Meteorological Years. Part I: South-Oriented Tilt Angles." *Applied Sciences* 11 (4): 1547–73.

Kambezidis, H. D., A. Farahat, M. Almazroui, and E. Ramadan. 2021. "Solar Potential in Saudi Arabia for Flat-Plate Surfaces of Varying Tilt Tracking the Sun." *Applied Sciences* 11 (23): 11564–86.

Klein, S. A. 1977. "Calculation of Monthly Average Insolation on Tilted Surfaces." *Solar Energy* 19 (4): 325–9.

Li, D. H. W., and T. N. T. Lam. 2007. "Determining the Optimum Tilt Angle and Orientation for Solar Energy Collection Based on Measured Solar Radiance Data." *International Journal of Photoenergy* 2007: Article ID 085402.

Liu, B. Y. H., and R. C. Jordan. 1963. "The Long-Term Average Performance of Flat-Plate Solar-Energy Collectors: With Design Data for the U.S, its Outlying Possessions and Canada." *Solar Energy* 7 (2): 53–74.

Mahmood, A. J. 2020. "Thermal Evaluation of a Double-Pass Unglazed Solar Air Heater with Perforated Plate and Wire Mesh Layers." *Sustainability* 12: 3619.

Mzad, H. 2008. "Prediction of Thermal Performance of Double-Glazed Solar Collector." *Archives of Thermodynamics* 29 (1): 69–84.

Mzad, H., A. Otmani, A. Haouam, S. Łopata, and P. Ocłoń. 2018. "Tilt Optimization of a Double-Glazed Air Solar Collector Prototype." *MATEC Web of Conferences* 240: 04006.

Mzad, H., K. Bey, and R. Khelif. 2019. "Investigative Study of the Thermal Performance of a Trial Solar Air Heater." *Case Studies in Thermal Engineering* 13: 100373.

Perez, R., P. Ineichen, R. Seals, J. Michalsky, and R. Stewart. 1990. "Modeling Daylight Availability and Irradiance Components from Direct and Global Irradiance." *Solar Energy* 44 (55): 271–89.

PVGIS database website. 2018. Also available at: https://re.jrc.ec.europa.eu/pvg_tools/fr/#MR.

Reindl, D. T., W. A. Beckman, and J. A. Duffie. 1990. "Evaluation of Hourly Tilted Surface Radiation Models." *Solar Energy* 45 (1): 9–17.

Saedodin, S., S. A. H. Zamzamian, M. E. Nimvari, S. Wongwises, and H. J. Jouybari. 2017. "Performance Evaluation of a Flat-Plate Solar Collector Filled with Porous Metal Foam: Experimental and Numerical Analysis." *Energy Conversion and Management* 153: 278–87.

Saxena, A., G. Srivastava, and V. Tirth. 2015. "Design and Thermal Performance Evaluation of a Novel Solar Air Heater." *Renewable Energy* 77: 501–11.

Soler, A., and K. K. Gopinathan. 1994. "Estimation of Monthly Mean Hourly Global Radiation for Latitudes in the 1°N–81°N Range." *Solar Energy* 52 (3): 233–9.

Tang, R., and T. Wu. 2004. "Optimal Tilt-Angles for Solar Collectors Used in China." *Applied Energy* 79 (3): 239–48.

Tiris, M., and C. Tiris. 1998. "Optimum Collector Slope and Model Evaluation: Case Study for Gebze, Turkey." *Energy Conversion and Management* 39 (3-4): 167–72.

Yadav, A. K., and S. S. Chandel. 2013. "Tilt Angle Optimization to Maximize Incident Solar Radiation: A Review." *Renewable and Sustainable Energy Reviews* 23: 503–13.